Received: 15 September 2023 | Revised: 31 October 2023 | Accepted: 4 November 2023

DOI: 10.1002/bit.28602

ARTICLE

BIOTECHNOLOGY AND BIOENGINEERING WILEY

Pushing the boundaries of phosphorylase cascade reaction for cellobiose production I: Kinetic model development

Alexander Sigg[1] | Mario Klimacek[1] | Bernd Nidetzky[1,2]

[1]Institute of Biotechnology and Biochemical Engineering, Graz University of Technology, NAWI Graz, Graz, Austria

[2]Austrian Centre of Industrial Biotechnology (ACIB), Graz, Austria

Correspondence
Bernd Nidetzky, Institute of Biotechnology and Biochemical Engineering, Graz University of Technology, NAWI Graz, Petersgasse 12, A-8010 Graz, Austria.
Email: bernd.nidetzky@tugraz.at

Funding information
Horizon 2020 Framework Programme

Abstract

One-pot cascade reactions of coupled disaccharide phosphorylases enable an efficient transglycosylation via intermediary α-D-glucose 1-phosphate (G1P). Such transformations have promising applications in the production of carbohydrate commodities, including the disaccharide cellobiose for food and feed use. Several studies have shown sucrose and cellobiose phosphorylase for cellobiose synthesis from sucrose, but the boundaries on transformation efficiency that result from kinetic and thermodynamic characteristics of the individual enzyme reactions are not known. Here, we assessed in a step-by-step systematic fashion the practical requirements of a kinetic model to describe cellobiose production at industrially relevant substrate concentrations of up to 600 mM sucrose and glucose each. Mechanistic initial-rate models of the two-substrate reactions of sucrose phosphorylase (sucrose + phosphate → G1P + fructose) and cellobiose phosphorylase (G1P + glucose → cellobiose + phosphate) were needed and additionally required expansion by terms of glucose inhibition, in particular a distinctive two-site glucose substrate inhibition of the cellobiose phosphorylase (from *Cellulumonas uda*). Combined with mass action terms accounting for the approach to equilibrium, the kinetic model gave an excellent fit and a robust prediction of the full reaction time courses for a wide range of enzyme activities as well as substrate concentrations, including the variable substoichiometric concentration of phosphate. The model thus provides the essential engineering tool to disentangle the highly interrelated factors of conversion efficiency in the coupled enzyme reaction; and it establishes the necessary basis of window of operation calculations for targeted optimizations toward different process tasks.

KEYWORDS

cascade bio-catalysis, cellobiose, disaccharide phosphorylases, indirect transglycosylation, mechanism-based kinetic modeling, substrate inhibition

Abbreviations: Cb, cellobiose; CbP, cellobiose phosphorylase; Fru, D-fructose; G1P, α-D-glucose 1-phosphate; Glc, D-glucose; Pi, phosphate; ScP, sucrose phosphorylase; Suc, sucrose.

1 | INTRODUCTION

Cascade bio-transformations based on multiple enzymatic reactions telescoped in one pot have drawn considerable attention in applied bio-catalysis research (An & Maloney, 2022; Benítez-Mateos et al., 2022; Kara & Rudroff, 2021; Pfeiffer & Nidetzky, 2023; Rosenthal et al., 2022; Ruales-Salcedo et al., 2019; Wu et al., 2021). The idea of an organic synthesis, realized by conversion of expedient substrates in several chemical steps without the isolation of intermediates, has strong appeal (Kara & Rudroff, 2021; Rosenthal & Lütz, 2018; Ruales-Salcedo et al., 2019; Schrittwieser et al., 2018; Sheldon & Brady, 2019). The view of biochemical engineering on enzyme cascades is however mixed (Burek et al., 2022; Kuschmierz et al., 2022; Nazor et al., 2021; Teshima et al., 2023). Advantage of economy in the processing steps used must be balanced against the drawback of expanse in process system complexity. The parameter space of process performance increases proportionally to the number of enzymatic steps included in the cascade reaction (Burgener et al., 2020; Siedentop et al., 2021). Numerous studies demonstrate cascade transformations for practical synthesis in principle (e.g., Nazor et al., 2021; Pfeiffer & Nidetzky, 2023), yet the true process boundaries, and the optimal window of process operation defined by them, often remain unexplored (Burek et al., 2022; Domínguez de María, 2021; Siedentop et al., 2021; Siedentop & Rosenthal, 2022; Wang et al., 2018).

Kinetic modeling is a powerful engineering tool for cascade reaction development (Kara & Rudroff, 2021; Petroll et al., 2019; Siedentop et al., 2021). In contrast to purely data driven approaches (Mandenius & Brundin, 2008; Siedentop et al., 2023; Villegas-Torres et al., 2018), it has the unique quality of offering a comprehensive description of the system behavior. Kinetic models enable systematic, knowledge-based approaches at optimization, owing to their ability to disentangle the complex network of interconnected factors of cascade process efficiency (Finnigan et al., 2019; Hold et al., 2016; Milker et al., 2017; for review, see Siedentop et al. 2021). Given this fundamental relevance of modeling, surprisingly, there seems to be a certain vagueness on its systematic use for practical effect in reaction development and optimization (for reviews, see Kara & Rudroff 2021; Siedentop et al., 2021). Analogous to experiment, kinetic models differ widely in the degree and detail of system description reached (Berendsen et al., 2006; Klimacek et al., 2020; Sigg et al., 2021; Sun et al., 2021). Central questions, like that of minimum model requirements for reliable application in cascade optimization, appear to lack authoritative answers. For non-specialists, therefore, the cost–benefit efficacy of kinetic modeling may often seem as not sufficiently concrete and clear. Eventually this can result in a major potential of an engineering tool not applied for the development.

Here, we studied the cascade transformation of two disaccharide phosphorylases for the production of cellobiose (Cb) from sucrose (Suc) and glucose (Glc) (Figure 1, Brucher & Häßler, 2019; Kitaoka et al., 1992a; Zhong et al., 2017). Although proposed by other authors in earlier works (Kitaoka et al., 1992a; Zhong et al., 2017), we avoided the use of glucose isomerase to convert the fructose (Fru) released from Suc into Glc. While attractive from the viewpoint of reaction economy, the glucose isomerase was not readily incorporated into the multienzyme system due its special requirements for immobilization and operating temperature (≥60°C) (di Cosimo et al., 2013). Moreover, while Glc was an expedient substrate and Fru considered as a valuable co-product of the overall reaction in context of sugar industry, the glucose isomerase would have added extra costs and complexity due to a third enzymatic reaction (Brucher & Häßler, 2019). We here show the systematic step-by-step development of a kinetic model of the two-enzyme one-pot process, based on a tightly interconnected approach of experiment and mathematical modeling. The development starts from a basal model that describes the minimum features of rate and equilibrium of the coupled reactions. This model is gradually expanded in a bottom-up fashion, as required to give a comprehensive description of dynamic system behavior under a wide range of conditions, including those considered for the industrial implementation (Brucher & Häßler, 2019). The cellobiose process analyzed here can serve to illustrate the importance of modeling for cascade reaction development in general. The stepwise approach used can provide important clarification on cascade reaction modeling deployed for an immediate practical use (Siedentop et al., 2021).

Cascade transformations by coupled phosphorylase reactions have promising applications in the production of carbohydrate commodities. The cellobiose process considered here is manufactured industrially for different uses in the food and feed sector (Brucher & Häßler, 2019; Kitaoka et al., 1992a). Glycosylation process technology based on glucose 1-phosphate intermediate (G1P; Figure 1) enables flexibility in the product scope of the biocatalytic production. Products synthesized by cascade approaches conceptually analogous to that of the cellobiose process (Figure 1) include glucosyl glycerol (Zhang et al., 2020), laminaribiose (Abi et al., 2019; Du et al., 2022), trehalose (Schwarz et al., 2007; Sun et al., 2021), cellodextrins (Ubiparip et al., 2020; Zhong et al., 2020), β-glucans (Bulmer et al., 2021; Ubiparip et al., 2021) and linear starch chains (Qi et al., 2014; Waldmann et al., 1986). The stepwise strategy of kinetic modeling presented here can thus be extended to the other phosphorylase systems. Except for works of Abi et al. (2019) and Zhong et al. (2017) on laminaribiose and cellobiose production, respectively, kinetic modeling has not been applied to these cascade reactions.

Cascade transformations comprised of two enzymatic reactions that are coupled by mutually shared substrate and product have a long tradition in applied biocatalysis (France et al., 2017; Schrittwieser et al., 2018; Sperl & Sieber, 2018). They are most prominently represented by nicotinamide coenzyme-dependent reactions of oxidoreductases that involve cycling of oxidized and reduced NAD(P) forms (Gandomkar et al., 2019; Goldberg et al., 2007). Given this well-known precedent, it is worthwhile to point out particular challenges involved in the development of phosphorylase cascade reactions. The amount of inorganic phosphate (Pi) supplied is generally substoichiometric to the other substrates used (e.g., sucrose and glucose in Figure 1). However, unlike true

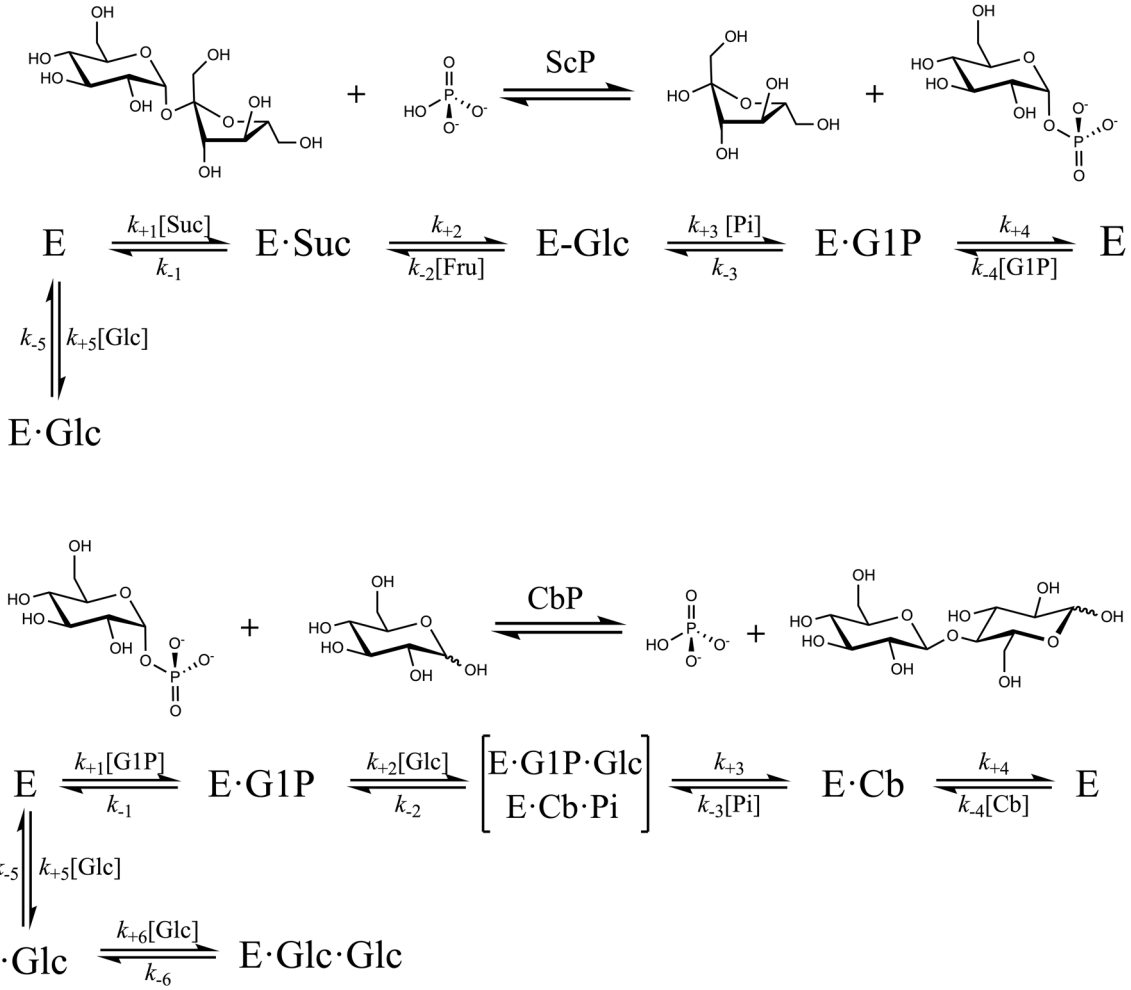

FIGURE 1 Kinetic mechanisms of ScP and CbP in the synthesis of cellobiose. ScP exhibits a competitive Glc-inhibition mechanism ($k_{\pm5}$) and CbP a dedicated two-site substrate inhibition by Glc ($k_{\pm5}$, $k_{\pm6}$).

co-substrates such as NAD(P), the phosphate and G1P concentrations needed for an efficient transformation are not just catalytic (Du et al., 2022; Zhong et al., 2017, 2019). The initial phosphate added thus becomes a complex factor of the conversion efficiency through its distributed effect on the maximum yield and the productivity of the individual reactions (Zhong & Nidetzky, 2020). The problem has also been recognized for reactions catalyzed by nucleoside phosphorylases (Giessmann et al., 2019; Kaspar et al., 2020). The here proposed kinetic model of cellobiose synthesis captures comprehensively the dynamic effect of the phosphate concentration under all conditions used.

2 | MATERIALS AND METHODS

2.1 | Materials, enzymes, assays

All chemicals were of highest reagent quality (Sigma-Aldrich; Carl Roth). *Bifidobacterium adolescentis* sucrose phosphorylase (ScP; GenBank identifier AF543301.1) and *Cellulomonas uda* cellobiose phosphorylase (CbP; GenBank identifier AAQ20920.1) were used as cell-free extract preparation from the respective *Escherichia coli* overexpression culture (Schwaiger et al., 2020). The specific activity of ScP was 47 U/mg, that of CbP was 11 U/mg. One unit (U) refers to 1 µmol/min of product released in the enzyme assay under the conditions used. Protein was determined with Bradford assay and bovine serum albumin as reference (Schwaiger et al., 2022). ScP activity was determined in a continuous coupled assay (250 mM sucrose, 50 mM phosphate) at 30°C and pH 7.0, as reported in Schwaiger et al. (2020) with measurement of NADH release and consecutive conversion into G1P concentrations as reported therein. CbP activity was determined in a discontinuous assay using 50 mM MES buffer (pH 7.0) at 30°C, measuring phosphate release (Sigg et al., 2021). Incubations (50 mM G1P, 80 mM glucose; 1.5 mL working volume) were done on a ThermoMixer C (Eppendorf) with agitation at 750 rpm. A temperature-controlled Beckman DU800 spectrophotometer was used for all spectroscopic assays.

2.2 | Inhibition studies

2.2.1 | Glc inhibition of CbP

Enzyme (0.17 U/mL) was incubated with 50 mM or 8.0 mM G1P in the presence of Glc varied at 80, 300, and 600 mM. Initial rates were determined from the phosphate release measured in five samples withdrawn at appropriate times up to 40 min (Klimacek et al., 2021).

2.2.2 | Glc inhibition of ScP

Enzyme preparation purified according to Sigg et al. (2021) was incubated at varied Suc concentration (0.5–100 mM) with Pi constant at 50 mM and Glc absent or present at a concentration of 10, 25, or 50 mM. The G1P release rate was determined in continuous measurements as for the enzyme assay (Schwaiger et al., 2020).

Data was fitted directly with Equation (1) for competitive inhibition, using nonlinear least-squares optimization in OriginPro 2019. In equation one, k_{cat} [1/s] refers to the turnover number, E [mM] to the enzyme concentration, v_{Suc} [mM/s] to the sucrose release rate under the tested steady state conditions, K_{Suc} [mM] to the Michaelis constant of Suc and K_{iGlc} [mM] to the inhibition constant of Glc.

$$v_{Suc} = \frac{k_{cat} \cdot [E] \cdot [Suc]}{K_{Suc}\left(1 + \frac{[Glc]}{K_{iGlc}}\right) + [Suc]} \quad (1)$$

2.3 | Reaction time course studies

Reactions were performed in 1.5 mL total volume using ThermoMixer C for agitation (750 rpm) and temperature control (30°C). A 50 mM MES buffer (pH 7.0) was used. The substrate concentrations varied in the range 100–600 mM (Suc, Glc) or 9–80 mM (Pi). The enzyme activities varied in the range 1.5–25 U/mL (ScP) and 0.75–8.9 U/mL (CbP). Samples (200 µL) were quenched in the same volume of buffer (99°C), further heat-inactivated in a boiling water bath for 10 min (Klimacek et al., 2020) and stored at −20°C until further analysis by HPLC. A Merck Hitachi L-7100 HPLC system (Merck) equipped with a YMC-Pack Polyamine II/S-5um/12 nm column and refractive index detection was used to analyze Fru, Glc, Suc and Cb. The column was operated at ambient temperature, with elution done at an isocratic flow (1 mL/min) of 75/25 acetonitrile/water (v/v) (Kruschitz & Nidetzky, 2020).

2.4 | Modeling methods

The King-Altman method (http://www.biokin.com/tools/king-altman/index.html) was used to derive rate equations for the kinetic mechanisms considered. Based on approach used in earlier works (Klimacek et al., 2020; Sigg et al., 2021), the microscopic rate constants were grouped into common kinetic parameters accessible to steady-state experiments. Kinetic models were fitted to time course data using COPASI 4.34 (Build 251) (Hoops et al., 2006). An evolutionary strategy with stochastic ranking (SERS) was used as optimization method (generations: 6000, population size: 20) for parameter estimation. Literature data on CbP (Nidetzky et al., 2000; Nidetzky et al., 2004) and ScP (Cerdobbel et al., 2011; Goedl et al., 2007; Sigg et al., 2021; Verhaeghe et al., 2013; Wildberger et al., 2011) were used to define upper and lower boundaries of the respective parameter estimate. Initial rate data acquired in this study served to implement additional fitting constraints. Moreover, the initial substrate and enzyme loadings were allowed to involve a relative error of ±5% and ±10%, respectively. The fitting involved randomized start values of parameters and the solver was allowed to perform at least 1.5×10^6 iterations until the objective value showed no further improvement. The procedure was repeated in 10 individual runs to evaluate parameter sensitivity (Klimacek et al., 2020; Sigg et al., 2021). Goodness of fit R^2 was calculated.

3 | RESULTS AND DISCUSSION

3.1 | Reaction time course analysis

The typical time course comprised seven sampling points, suitably distributed to cover the initial reaction phase as well as the approach to the reaction equilibrium (see Figure 2). As shown in Table 1, five conditions were selected for model fit and four additional conditions were used for model validation. The reactants analyzed (Suc, Glc, Fru, Cb) were sufficient for determination of the mass balance. Pi and G1P were occasionally measured for additional verification. The results shown are internally consistent based on close mass balance. High substrate concentrations (≥100 mM) were chosen for industrial relevance. Brucher and Häßler (2019) reported Cb production from 600 mM of each Suc and Glc as an industrial test case. As in a realistic process scenario, Suc and Glc were generally used at the same concentration to enable high conversion of both substrates. Departure from the standard Suc/Glc ratio was used to challenge the model for fit and validation. The Pi concentrations were selected to cover different degrees of saturation of the ScP (K_{Pi} = 19.3 mM), both initially and during the reaction. The ScP/CbP activity ratio varied between 2.0 and 10, with CbP changing in a 10-fold range (0.75–8.9 U/mL). The ScP was used in excess to ensure efficient supply of G1P to the CbP reaction. Note: the specific activity of ScP in the cell extract preparation of enzyme used surpasses that of CbP by 4.7-fold (Schwaiger et al., 2022). In the purified enzymes, the difference in specific activity is as large as 10-fold (Schwaiger et al., 2022).

Experimental results used in model fitting are summarized in Figure 2. Distribution of the initial Pi into G1P released during the reaction was obtained from direct measurements or it was calculated from the mass balance. The [G1P] (=[Fru]-[Cb]) approached the maximum of Pi used in the different reactions,

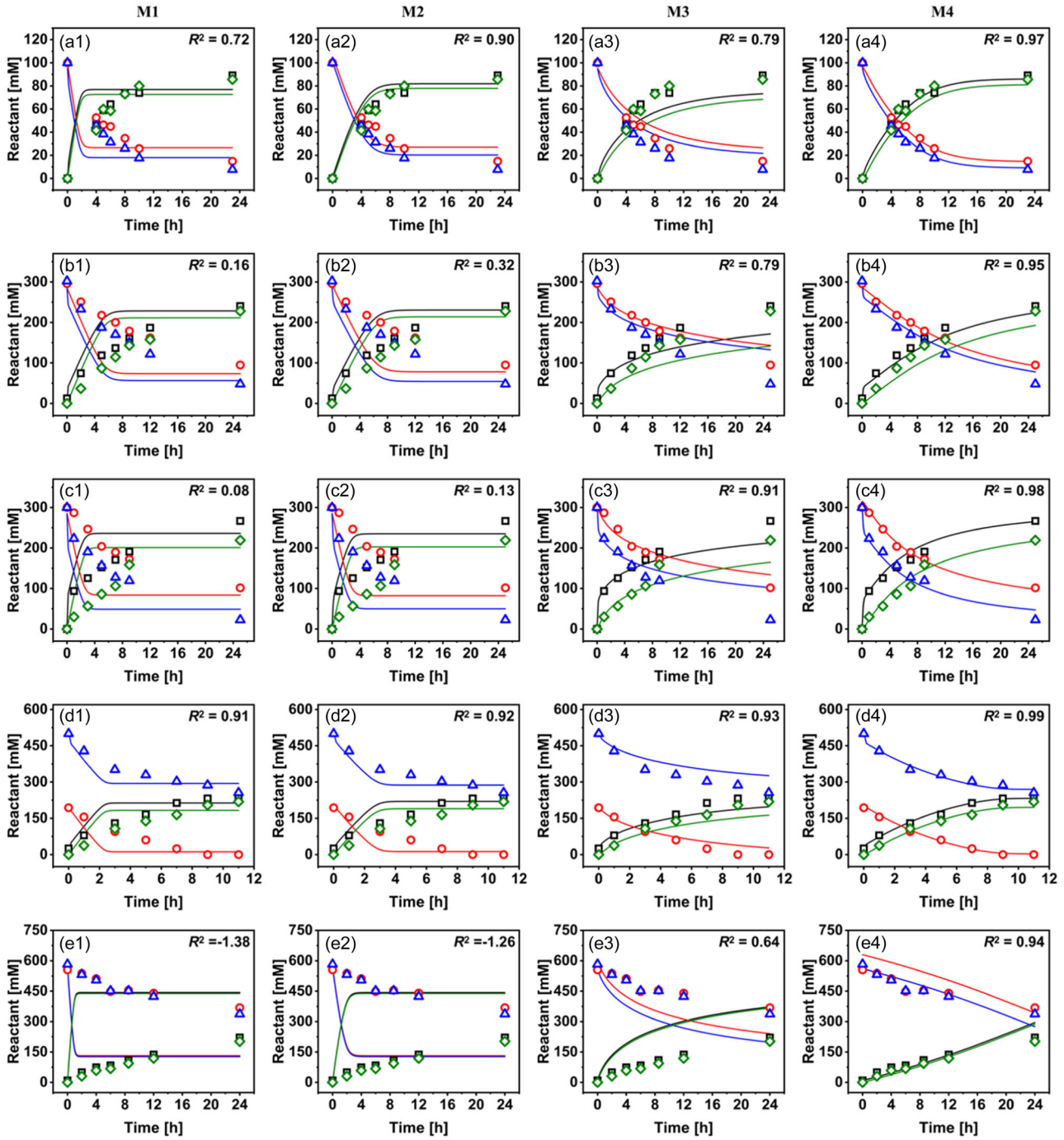

FIGURE 2 Summary of results obtained from experimental time-course analysis and parameter estimation by modeling. Symbols show the data (Suc, triangles; Glc circles; Fru, squares; Cb, diamonds), lines the best fit result of the respective kinetic model with goodness of fit (R^2) indicated. Initial reaction conditions are summarized in Table 1 (experimental) and Supporting Information Table S6 (modeling). Labeling of the panels of this Figure with (a–e) indicates the experimental conditions A–E, respectively, of the Model fit section of Table 1 used. The numbers 1–4 are for fits with model M1–M4, respectively.

indicating that recycling of the intermediary G1P was effectively achieved under all conditions used. Except for the 600 mM reaction (experiment E), equilibrium was approached in all reactions after 24 h of incubation. The reaction containing 600 mM Suc was unusually slow, providing a first indication of inhibition by high substrate concentration. Figure 2 serves to illustrate a main point of this study, that optimization of the cascade reaction based on experiment alone constitutes an extremely challenging task. The difficulty arises not only from the extensive experimentation necessary, but also fundamentally from the requirement to represent a highly interconnected system of process factors and metrics in a suitable experimental design.

TABLE 1 Initial conditions used in experimental time course studies.

		Model fit					Model validation			
Parameter	Unit	A	B	C	D	E	A	B	C	D
ScP	[U mL^{-1}]	1.50	7.77	11.6	11.6	25.2	1.18	9.72	11.6	11.6
CbP	[U mL^{-1}]	0.75	0.75	1.52	1.52	8.93	0.76	1.52	1.52	1.52
[Suc]	[mM]	100	300	300	500	600	100	300	300	200
[Glc]	[mM]	100	300	300	200	600	100	300	300	500
[Pi]	[mM]	9.1	39	80	39	10	9.1	39	71	39

TABLE 2 Kinetic models of the coupled reaction of ScP and CbP.[a]

Model M1	
ScP:	$v = V_f\left(1 - \frac{\Gamma}{K_{eq}}\right), \Gamma = \frac{[G1P][Fru]}{[Suc][Pi]}$
CbP:	$v = V_f\left(1 - \frac{\Gamma}{K_{eq}}\right), \Gamma = \frac{[Pi][Cb]}{[G1P][Glc]}$
Model M2	
ScP:	$v = \frac{V_f[Suc][Pi]}{K_{Suc}[Pi] + K_{Pi}[Suc] + [Suc][Pi]}\left(1 - \frac{\Gamma}{K_{eq}}\right), \Gamma = \frac{[G1P][Fru]}{[Suc][Pi]}$
CbP:	$v = \frac{V_f[G1P][Glc]}{K_{iG1P}K_{Glc} + [G1P][Glc] + K_{G1P}[Glc] + K_{Glc}[G1P]}\left(1 - \frac{\Gamma}{K_{eq}}\right), \Gamma = \frac{[Pi][Cb]}{[G1P][Glc]}$
Model M3	
ScP:	$v = \frac{V_f[Suc][Pi]}{K_{Suc}[Pi] + K_{Pi}[Suc] + [Suc][Pi]}\left(1 - \frac{\Gamma}{K_{eq}}\right), \Gamma = \frac{[G1P][Fru]}{[Suc][Pi]}$
CbP:	$v = \frac{V_f[G1P][Glc]}{D}\left(1 - \frac{\Gamma}{K_{eq}}\right), \Gamma = \frac{[Pi][Cb]}{[G1P][Glc]}$ $D = K_{iG1P}K_{Glc}\left(1 + \frac{[Glc][Pi][Cb]}{K_{iCb}K_{Pi}K_{iGlc1}} + \frac{[Pi][Cb]}{K_{iCb}K_{Pi}} + \frac{K_{Cb}[Glc][Pi]}{K_{iCb}K_{Pi}K_{iGlc2}} + \frac{K_{Cb}[Pi]}{K_{iCb}K_{Pi}} + \frac{[Cb]}{K_{iCb}}\right)$ $+ \frac{[G1P][Glc][Pi]}{K_{iPi}} + K_{Glc}[G1P]\left(1 + \frac{K_{Cb}[Pi]}{K_{iCb}K_{Pi}}\right) + [G1P][Glc]$
Model M4	
ScP:	$v = \frac{V_f[Suc][Pi]}{K_{Suc}[Pi]\left(1 + \frac{[Glc]}{K_{iGlc}}\right) + K_{Pi}[Suc] + [Suc][Pi]}\left(1 - \frac{\Gamma}{K_{eq}}\right), \Gamma = \frac{[G1P][Fru]}{[Suc][Pi]}$
CbP:	$v = \frac{V_f[G1P][Glc]}{D}\left(1 - \frac{\Gamma}{K_{eq}}\right), \Gamma = \frac{[Pi][Cb]}{[G1P][Glc]}$ $D = K_{iG1P}K_{Glc}\left(1 + \frac{[Glc][Pi][Cb]}{K_{iCb}K_{Pi}K_{iGlc1}} + \frac{K_{Cb}[Glc]^2[Pi]}{K_{iCb}K_{Pi}K_{iGlc2}K_{iGlc3}} + \frac{[Pi][Cb]}{K_{iCb}K_{Pi}}\right.$ $\left. + \frac{K_{Cb}[Glc][Pi]}{K_{iCb}K_{Pi}K_{iGlc2}} + \frac{[Glc]^2}{K_{iGlc2}K_{iGlc3}} + \frac{K_{Cb}[Pi]}{K_{iCb}K_{Pi}} + \frac{[Cb]}{K_{iCb}} + \frac{[Glc]}{K_{iGlc2}}\right)$ $+ K_{G1P}[Glc]\left(1 + \frac{[Glc]^2}{K_{iGlc2}K_{iGlc2}} + \frac{[Cb]}{K_{iCb}} + \frac{[Glc]}{K_{iGlc2}}\right) + \frac{[G1P][Glc][Pi]}{K_{iPi}}$ $+ K_{Glc}[G1P]\left(1 + \frac{K_{Cb}[Pi]}{K_{iCb}K_{Pi}}\right) + [G1P][Glc]$

Abbreviations: Cb, cellobiose; Fru, fructose; G1P, α-D-glucose 1-phosphate; Glc, glucose; K, Michaelis constant; K_i, dissociation constant; K_{eq}, equilibrium constant; Pi, phosphate; Suc, sucrose; V_f, maximum velocity of the forward direction.

[a]Definition of kinetic parameters is provided in Table S1 in Supporting Information.

3.2 | Flux models M1 and M2

Engineering approach to kinetic model development involves parsimony of parameterization as a guiding principle (Almquist et al., 2014; Gernaey et al., 2010; Lauterbach et al., 2023; Lencastre Fernandes et al., 2013; Sadino-Riquelme et al., 2020). Considering a bottom-up strategy of stepwise increase in model complexity, the minimum feature of basal model is that of an enzymatic net rate (flux) under control of mass action. The relevant models are identified as M1 and M2 in Table 2 with respective kinetic parameters being defined in Table S1 in the Supporting Information. Both models do not consider effects of the back reaction on the forward flux

introduced by reversible binding of released products. Generally, therefore, they are expected to be particularly suitable for reactions with equilibrium far on the product side. The conditions are met by the ScP (Goedl et al., 2007; Wildberger et al., 2011) and CbP (Nidetzky et al., 2004) reactions in the directions considered for Cb production (Table 1). Model M1 assumes zero-order kinetics with respect to all substrates. Despite this major simplification, model M1 is a useful starting point for the development of a kinetic model, in particular because its use requires only the two central parameters of each reaction: a specific rate (activity) of the enzyme and an equilibrium constant. As shown in Figure 2, model M1 describes adequately the reaction equilibrium for all reactions except that at 600 mM, but the dynamic approach to the equilibrium is not captured well. The model predicted reaction progress in the initial phase of conversion to be much faster (≥3-fold) than in the experiment. Conclusion at this point is that enzymes are not fully saturated with both their substrates under conditions of the coupled reaction and a successful model must adequately account for that fact. The in situ recycled substrates Pi and G1P are likely limiting for the ScP and CbP reactions, respectively. Equilibrium constants and initial parameters predicted for model M1 are shown in Tables S2 and S6 (Supporting Information), respectively.

Model M2 thus expands model M1 by including a mechanism-based description of the substrate concentration dependence of the enzymatic forward rates. Figure 1 identifies the bisubstrate kinetic mechanism of ScP as Ping-Pong Bi-Bi (Mirza et al., 2006), that of CbP as Ordered Bi-Bi (Nidetzky et al., 2000). Note that steps of product binding or inhibition are also shown in Figure 1 but are not included in model M2. Change from model M1 to M2 involves substantial increase in the parameters used. For ScP and CbP, these parameters were available from literature (ScP: Cerdobbel et al., 2011; Goedl et al., 2007; Sigg et al., 2021; Verhaeghe et al., 2013; Wildberger et al., 2011, CbP: Nidetzky et al., 2000; Nidetzky et al., 2004). In situations of enzyme kinetic parameters not available, simplified versions of model M2 (see the Supporting Information Table S1) could be considered in a first step to economize the parameter use in model development (for use of so-called "convenience models", see Liebermeister and Klipp, 2006).

Compared with model M1, model M2 gives a clear improvement in the fit of data (Figure 2). The time course at 100 mM substrate is well represented in full. At the higher substrate concentrations, however, the deviation between model M2 fit and experiment is still pronounced, especially in the early reaction phase. The initial production rates are overestimated by up to 7.3-fold by the model (Figure 2e2). Parameter estimates (Table S3) and other constraints (Table S6) are generally found at the upper or lower boundary, suggesting the overall fit to have been problematic. Rate-retarding effects seen at elevated substrate concentrations are clearly not due to a single factor, such as the product concentration released. They appear to arise from a complex interplay of factors related to the substrate concentration itself, the product concentration released from it, and the phosphate concentration used. Comparison of Figure 2b2–e2 illustrates the point. The Cb product concentration is almost the same in all reactions (~210 mM), yet the discrepancy between model fit and experiment differs largely among the reactions, for example, b2 and e2.

The results imply that effects of product binding on the net forward rate must be included in the kinetic model. Here in particular for CbP, one expects competition for binding to the free enzyme by the accumulating Cb with the G1P present at a much lower steady-state concentration. The situation is opposite for ScP because the Suc present in large excess outcompetes completely the G1P for binding to the free enzyme. The accumulating Fru might compete with Pi for binding to the glucosylated enzyme intermediate. However, there is good evidence that the half-reaction with Suc (Figure 1) is rate-limiting (Vyas & Nidetzky, 2023). At saturating [Suc], therefore, the enzyme complex with Suc is the predominant form of ScP present at steady state. Based on these considerations, therefore, we added terms of reaction reversibility only to the kinetic model of CbP.

3.3 | Reversible model M3

The expanded model M3 is shown in Table 2 with kinetic parameters being defined in Table S1 (Supporting Information). The fitting results are shown in Figure 2a3–e3 and the associated parameters are summarized in Tables S4 and S6 (Supporting Information). Improved fit by model M3 compared with M2 is seen by increase in R^2 in all reactions, interestingly with the exception of the 100 mM reaction. Despite that, model M3 involves the bias that Cb release in the initial reaction phase is underestimated (~35%) at low substrate concentration (Figure 2a3) while it is overestimated (~70%) at high substrate concentration (Figure 2e3). The observed trend suggests that the substrate becomes inhibitory when used at high concentration. Model M3 does not incorporate substrate inhibition. The Glc substrate is a known inhibitor of both enzymes in general (ScP: Mieyal and Abeles, 1972; CbP: Rajashekhara et al., 2002). For the ScP from *B. adolescentis* and CbP from *C. uda* used here, inhibition by Glc has not been characterized. Close inspection of trend comprised in the time course data leads to the conclusion that Glc exercises inhibition significantly whereas an inhibitory effect of Suc is negligible in comparison, as follows. Reaction d3 involves increase in [Suc] by 200 mM but decrease in [Glc] by 100 mM compared with reaction b3. Judged by R^2, model M3 fits reaction d3 better than reaction b3, inconsistent with a dominant role of inhibition by Suc. By the same criterion of R^2 value, model M3 fits reaction e3 by far less well than it fits reaction d3. Increase by 400 mM in the [Glc] used is the most prominent among the changes in condition between reaction e3 and d3. In summary, therefore, these results strongly supported the suggestion to examine Glc inhibition in more detail.

3.4 | Glc inhibition and development of model M4

The characterizations done were based on earlier studies of related enzymes. The Glc inhibition of ScP is competitive against Suc (Mieyal & Abeles, 1972) and involves Glc binding to the sugar-binding subsite−1 of the enzyme (Mirza et al., 2006). As shown in Figure 3a that presents data in the form of a double reciprocal plot, ScP exhibits the same type of inhibition. Nonlinear fit gives an inhibition constant (K_{iGlc}) of 3.43 ± 0.18 mM with an associated Michaelis constant for Suc (K_{Suc}) of 0.82 ± 0.04 mM.

The Glc inhibition of CbP arises from Glc binding to both sugar binding subsites of the enzyme (Figure 1; Kitaoka et al., 1992b). The two-site binding mode results in a rather unusual type of substrate inhibition by Glc, as shown in Figure 3b based on data acquired for CbP. Full-fledged inhibition study of CbP was considered beyond the scope of the current work. The integrated approach used here involved parameters of the Glc inhibition ($K_{iGlc2} = k_{-5}/k_{+5}$; $K_{iGlc3} = k_{-6}/k_{+6}$; see Figure 1 for assignment of microscopic rate constants to respective kinetic steps) included into the kinetic model M4 and parameter estimates obtained from global fits of the model to the time course data. The initial rate data of Figure 3b served as additional constraints.

The model M4 is shown in Table 2 with kinetic parameters being defined in Table S1 (Supporting Information). Fitting was done with K_{iGlc3} (the constant for Glc binding to sugar-binding subsite +1) as variable parameter for estimation or held constant at 10^{20} mM to exclude effect of inhibition at this site. Model M4 with the restriction of invariant K_{iGlc3} is incapable of reproducing all the time courses (Figure S1a–e, Supporting Information), nor does it represent the initial-rate inhibition data of the CbP (Figure S1f, Supporting Information). The full model M4 with K_{iGlc3} determined from fit, however, gives an excellent description of the whole data set in time courses (Figure 2a4–e4) and initial rates (Figure 3b). The fitted parameters are summarized in Tables S5 and S6 (Supporting Information). Covariance analysis reveals that estimates of K_{iGlc2} and K_{iGlc3} are inversely correlated with a correlation coefficient close to −1. This shows the impossibility of independent estimation of the two parameters from model M4 fits to the available data set. The estimated values in Table S5 are used with caution as they may have converged to extremes. However, the inhibition data in Figure 3b can be represented with excellent accuracy with various combinations of K_{iGlc2} and K_{iGlc3}.

Model 4 validation is presented in Figure 4 that shows simulation results compared with a fresh set of time course data (Table 1). The scope of model M4 applicability is challenged strongly by the validation data as they represent changes in the enzyme ratio (Figure 4a,b), the Pi concentration (Figure 4a–c) and the ratio of substrate concentrations used (Figure 4d) in comparison to the data used for fitting. Judged by the value of R^2, the agreement between simulation and experiment is excellent ($R^2 \geq 0.95$; Figure 4b–d). The 100 mM reaction (Figure 4a) is an exception ($R^2 = 0.67$). Lowering of R^2 in Figure 4 compared with Figure 2a4–e4 is understood, in general, to arise from the fact that simulations use fixed loadings of enzyme and substrate while fittings allow error in these loadings. Ability of model M4 to reproduce the reaction in Figure 4d where Glc (500 mM) was used in 2.5-fold excess over Suc supports the earlier conclusion from fits of model M3 that inhibition by Suc is insignificant.

3.5 | Bottom-up construction of kinetic model of enzyme cascade reaction

Kinetic model M4 is presented for phosphorylase cascade synthesis of cellobiose under conditions of high substrate concentration relevant for the industrial production. Accompanying paper shows flexible use of the kinetic model for optimization of different processing tasks in cellobiose production (Sigg et al., 2023). The

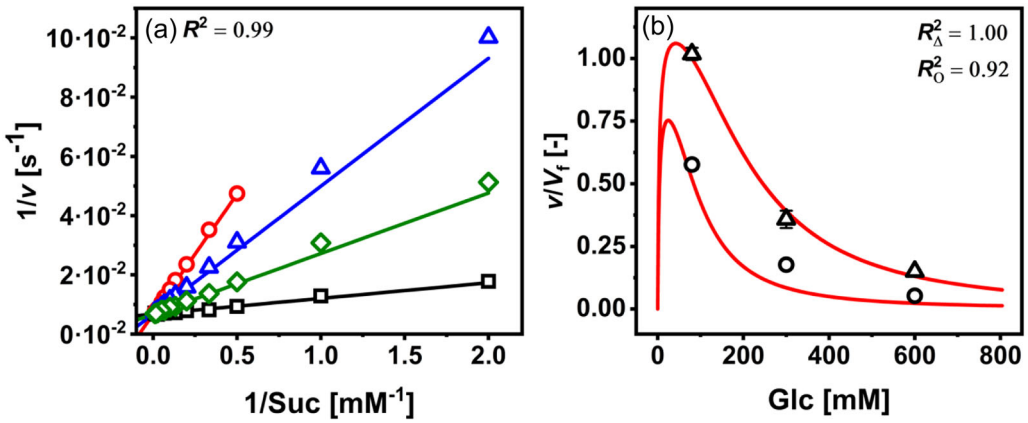

FIGURE 3 Results of inhibition analysis for ScP (a) and CbP (b). (a) Symbols show the experimental data ([Pi] = 50 mM with [Glc] applied at 50 mM, circles; 25 mM, triangles; 10 mM, diamonds; 0 mM, squares), and solid lines show the best fit result. (b) Symbols show experimental data (triangles, [G1P] = 50 mM; circles [G1P] = 8 mM). Solid lines show the data overlay of $N = 10$ fitting experiments using model M4, with goodness of fit R^2 indicated for the best fit result. Experimental data are averages ($N = 2$) and error bars show the corresponding standard deviation.

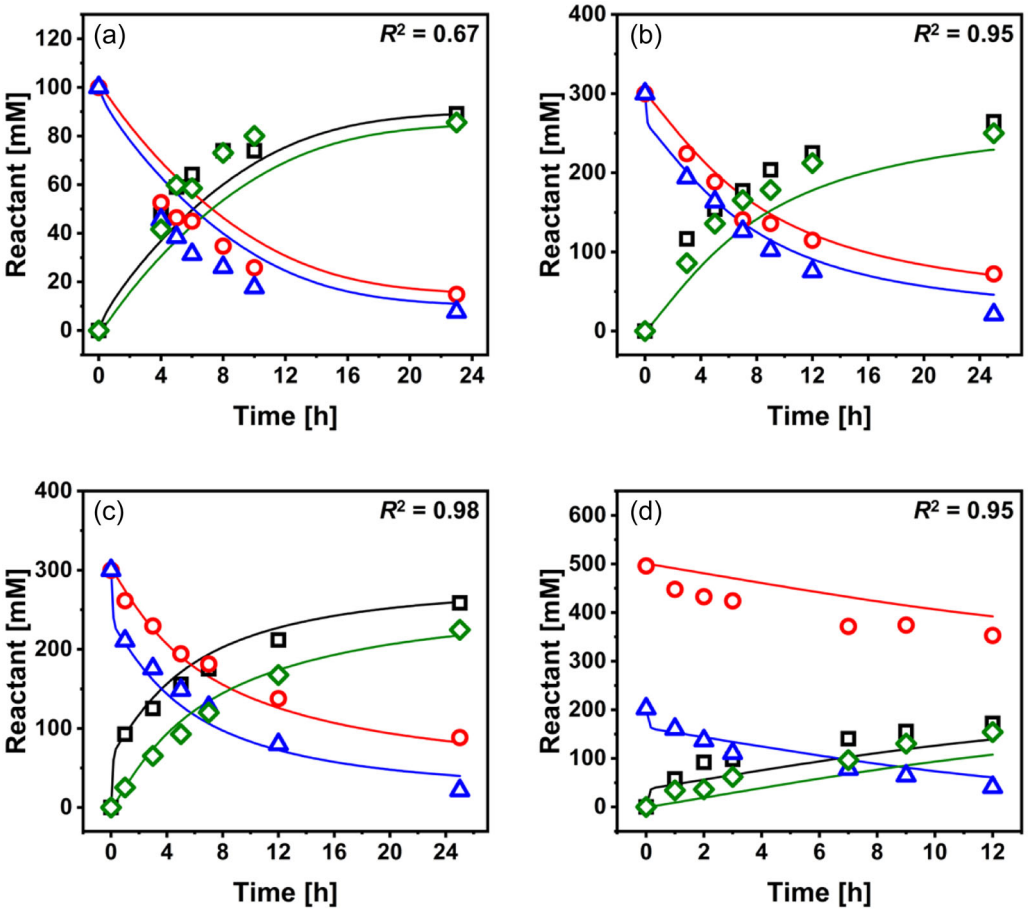

FIGURE 4 Validation of model M4. Lines show the prediction of reaction time courses, symbols the experimental data (Suc, triangles; Glc circles; Fru, squares; Cb, diamonds), with goodness of fit (R^2) indicated. The labeling of the panels (a–d) of this figure indicates the experimental conditions A–D, respectively, of the Model validation section of Table 1 used.

kinetic model enables a broad range of optimization problems to be addressed in a fully quantitative analysis. Its scope of application in process development is therefore distinct from that accessible via solely data-driven approaches (for general review, see Helleckes et al., 2023; Mandenius & Brundin, 2008; Schulze & Schenkendorf, 2020; Siedentop et al., 2021)

The systematic step-by-step development of model M4 from the basal flux model M1 informs kinetic model development for enzyme cascade transformations in general (Kara & Rudroff, 2021). In particular, the bottom-up approach of model construction used yields a reasoned assessment of the complexity required of the successful kinetic model. Readers may find model M4 exceedingly involved in the mathematical description used. It can be illuminating, therefore, to compare the reactions of CbP and ScP. The cellobiose synthesis from G1P and Glc exhibits complex kinetic behavior indeed. We provide evidence for the essentiality that this complexity is implemented in full for the kinetic model to be able to describe the enzymatic reaction in a realistic range of operating conditions. However, the relatively simple flux model M2, only expanded to include competitive inhibition by Glc, is fully sufficient to describe phosphorolysis of Suc in the presence of Pi. Considering the differences in kinetics of the two phosphorylase reactions, a few general guidelines for systematic approach to model development for coupled enzyme cascade reaction can be formulated (Figure 5).

We begin with the reasonable assumption that equilibrium constants of the individual reactions are known from experiment or have plausible estimates from computational analysis (Beber et al., 2022). Approach of reaction to equilibrium is thus described by mass action term. Additionally, we assume that an apparent K value (obtained from experiments done at saturating concentrations of the respective other substrate) is available. In conditions of $[S_0]/K$ greater than 10 and K_{eq} strongly favoring the formation of the products, flux model M1 might give an adequate description of the data. Dependence of the rate on the substrate concentration (flux models of the M2 type) can be implemented stepwise for each substrate with empirical (hyperbolic) terms (Liebermeister & Klipp, 2006). The model based on the enzyme kinetic mechanism is most accurate to describe the rate at low substrate concentrations. In modeling coupled enzyme reactions, the important decision on whether an empirical or mechanism-based kinetic model of M2 type is required depends primarily on the steady-state concentrations of the recycled substrates during the transformation, relative to the corresponding K of the enzyme. In the phosphorylase cascade reaction under the conditions

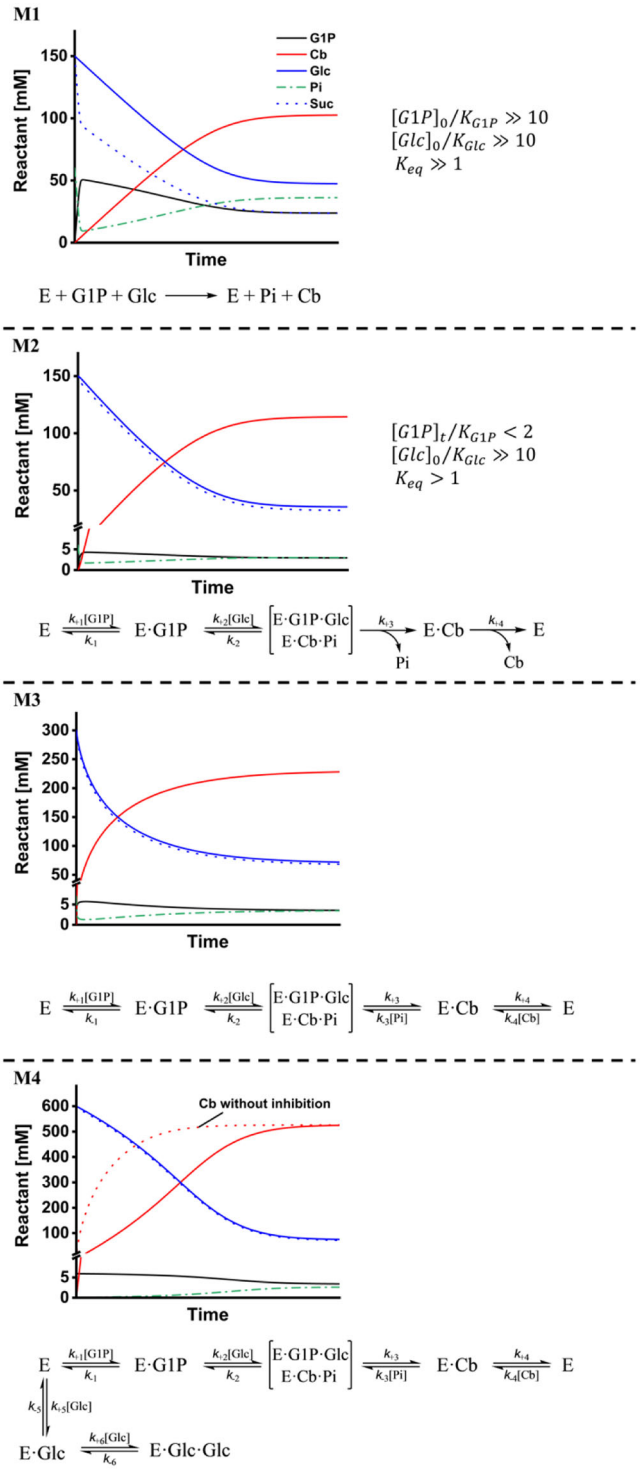

FIGURE 5 Bottom-up development of kinetic model for describing enzyme cascade reactions.

used here, the enzymes are not fully saturated with Pi and G1P at the respective concentrations available in the process. The situation of recycled substrate or intermediate present in non-saturating concentration will probably occur often in enzyme cascade reactions. Considering economy of experiment, our recommendation is to examine the empirical description first because it requires a smaller set (~10-fold) of initial rate data for parameter estimation than the mechanistic description. In the current study, parameters of mechanistic kinetic model were available for both enzymes from literature. Their implementation as additional constrains (lower and upper boundaries) for model fitting ensure mechanistic correctness and provides basis for the evaluation of model accuracy.

Model extension to include reaction reversibility (model type M3) is possible on both empirical and mechanistic types of the M2 model, effectively resulting in the inclusion of product inhibition terms. In a two-step cascade transformation, it is always the second step (the one requiring the intermediate as the substrate) that experiences the stronger effect. The product released accumulates to a high concentration while the substrate remains at the comparably low steady-state concentration. Lastly, particular forms of substrate inhibition can be included to obtain models of type M4. In phosphorylase cascade reactions for disaccharide and oligosaccharide production (e.g., Du et al., 2022; Qi et al., 2014; Zhong et al., 2020), the substrates used and the product released exhibit structural similarity to a considerable degree. The possibility of cross-inhibition (e.g., ScP inhibition by glucose) must therefore be considered. A limited set of initial rate experiments is here however sufficient to identify the relevant inhibitions. Parameter estimation is then possible directly from model fit to the experimental time courses. Earlier efforts at modeling phosphorylase cascade reactions are noted (Abi et al., 2018; Sun et al., 2021; Zhong et al., 2017). However, these studies presumed the requirement of a particular model structure and degree of parametrization. Lacking the stepwise approach to an increased model complexity as used here, models may suffer from the exclusion of effects requiring description while other effects, described by the model, are overparametrized. In particular, the model of Zhong et al. (2017) describing cellobiose production lacked detailed information of the mechanism of substrate and product inhibition and therefore demanded additional adjustment of kinetic parameters to values exceeding experimental observation.

4 | CONCLUSION

Kinetic model-based reaction optimization is generally recognized for its critical importance in biocatalytic process development and scale up. Central problem of the kinetic modeling approach is to identify minimum requirements of a practically useful model in terms of model structure and detail. In particular, the fundamental question arises inhowfar the model must represent certain features of the enzyme kinetic mechanism to describe dynamic reaction behavior with sufficient accuracy under the relevant process conditions. We here show the systematic (step-by-step) bottom-up development of kinetic model for the coupled ScP-CbP reaction applied to Cb production. The overall approach of model construction is general and so can have relevance for others working with biocatalytic cascade reactions. We demonstrate the requirement for a full-fledged mechanistic model to describe the steady-state kinetics of CbP, affected by an unusual two-site substrate inhibition of Glc and product inhibition of Cb. Evidence that the ScP reaction was described

sufficiently by a much simpler kinetic model underlines the importance of a bottom-up process of kinetic model construction. This process, as shown for CbP, may involve the transition from empirical to mechanistic kinetic model as a key step of the development. The kinetic model of the coupled ScP-CbP reaction provides a powerful engineering tool for the analysis and optimization of the overall conversion in dependence of the various interrelated factors of process performance (e.g., substrate and enzyme concentrations and ratios thereof) that it would be impossible to disentangle by human intuition alone. The model thus identifies boundaries on transformation efficiency that result from kinetic and thermodynamic characteristics of the individual enzyme reactions. The optimization of G1P supply is challenging in particular because it involves a significant trade-off between kinetics (rate, productivity) and thermodynamics (yield). The phosphate concentration used is substoichiometric to Suc, but due to K_m values for Pi and G1P in the mM range, it cannot be so strictly catalytic as, for example, the nicotinamide coenzyme concentrations (typically < 1 mM) in dehydrogenase cascade reactions. Accompanying paper shows application of the kinetic model for window of operation calculations to enable targeted optimizations of ScP-CbP reaction toward different process tasks.

ACKNOWLEDGMENTS

This project has received funding from the European Union's Horizon 2020 research and innovation program under grant agreement No. 761030 (CARBAFIN).

DATA AVAILABILITY STATEMENT

Data of the current study are available from DOI 10.5281/zenodo.6956069.

ORCID

Bernd Nidetzky http://orcid.org/0000-0002-5030-2643

REFERENCES

Abi, A., Hartig, D., Vorländer, K., Wang, A., Scholl, S., & Jördening, H.-J. (2019). Continuous enzymatic production and adsorption of laminaribiose in packed bed reactors. *Engineering in Life Sciences*, *19*(1), 4–12. https://doi.org/10.1002/elsc.201800110

Abi, A., Wang, A., & Jördening, H.-J. (2018). Continuous laminaribiose production using an immobilized bienzymatic system in a packed bed reactor. *Applied Biochemistry and Biotechnology*, *186*(4), 861–876. https://doi.org/10.1007/s12010-018-2779-2

Almquist, J., Cvijovic, M., Hatzimanikatis, V., Nielsen, J., & Jirstrand, M. (2014). Kinetic models in industrial biotechnology—Improving cell factory performance. *Metabolic Engineering*, *24*, 38–60. https://doi.org/10.1016/j.ymben.2014.03.007

An, C., & Maloney, K. M. (2022). Designing for sustainability with biocatalytic and chemoenzymatic cascade processes. *Current Opinion in Green and Sustainable Chemistry*, *34*, 100591. https://doi.org/10.1016/j.cogsc.2022.100591

Beber, M. E., Gollub, M. G., Mozaffari, D., Shebek, K. M., Flamholz, A. I., Milo, R., & Noor, E. (2022). eQuilibrator 3.0: A database solution for thermodynamic constant estimation. *Nucleic Acids Research*, *50*(D1), D603–D609. https://doi.org/10.1093/nar/gkab1106

Benítez-Mateos, A. I., Roura Padrosa, D., & Paradisi, F. (2022). Multistep enzyme cascades as a route towards green and sustainable pharmaceutical syntheses. *Nature Chemistry*, *14*(5), 489–499. https://doi.org/10.1038/s41557-022-00931-2

Berendsen, W. R., Gendrot, G., Freund, A., & Reuss, M. (2006). A kinetic study of lipase-catalyzed reversible kinetic resolution involving verification at miniplant-scale. *Biotechnology and Bioengineering*, *95*(5), 883–892. https://doi.org/10.1002/bit.21034

Brucher, B., & Häßler, T. (2019). Enzymatic process for the synthesis of cellobiose. In A. Vogel & O. May (Eds.), *Industrial enzyme applications*. Wiley-VCH Verlag GmbH & Co. KGaA. https://doi.org/10.1002/9783527813780.ch2_4

Bulmer, G. S., de Andrade, P., Field, R. A., & van Munster, J. M. (2021). Recent advances in enzymatic synthesis of β-glucan and cellulose. *Carbohydrate Research*, *508*, 108411. https://doi.org/10.1016/j.carres.2021.108411

Burek, B. O., Dawood, A. W. H., Hollmann, F., Liese, A., & Holtmann, D. (2022). Process intensification as game changer in enzyme catalysis. *Frontiers in Catalysis*, *2*, 858706. https://doi.org/10.3389/fctls.2022.858706

Burgener, S., Luo, S., McLean, R., Miller, T. E., & Erb, T. J. (2020). A roadmap towards integrated catalytic systems of the future. *Nature Catalysis*, *3*(3), 186–192. https://doi.org/10.1038/s41929-020-0429-x

Cerdobbel, A., De Winter, K., Aerts, D., Kuipers, R., Joosten, H.-J., Soetaert, W., & Desmet, T. (2011). Increasing the thermostability of sucrose phosphorylase by a combination of sequence- and structure-based mutagenesis. *Protein Engineering, Design and Selection*, *24*(11), 829–834. https://doi.org/10.1093/protein/gzr042

Di Cosimo, R., McAuliffe, J., Poulose, A. J., & Bohlmann, G. (2013). Industrial use of immobilized enzymes. *Chemical Society Reviews*, *42*, 6437–6474. https://doi.org/10.1039/C3CS35506C

Domínguez de María, P. (2021). Biocatalysis, sustainability, and industrial applications: Show me the metrics. *Current Opinion in Green and Sustainable Chemistry*, *31*, 100514. https://doi.org/10.1016/j.cogsc.2021.100514

Du, Z., Li, F., Liu, Z., Tan, Y., Niu, K., & Fang, X. (2022). Driving an in vitro multienzymatic cascade of laminaribiose biosynthesis from non-food cellulose with balancing the precursor supply. *Industrial Crops and Products*, *182*, 114878. https://doi.org/10.1016/j.indcrop.2022.114878

Finnigan, W., Cutlan, R., Snajdrova, R., Adams, J. P., Littlechild, J. A., & Harmer, N. J. (2019). Engineering a seven enzyme biotransformation using mathematical modelling and characterized enzyme parts. *ChemCatChem*, *11*(15), 3474–3489. https://doi.org/10.1002/cctc.201900646

France, S. P., Hepworth, L. J., Turner, N. J., & Flitsch, S. L. (2017). Constructing biocatalytic cascades: In vitro and in vivo approaches to de novo multi-enzyme pathways. *ACS Catalysis*, *7*(1), 710–724. https://doi.org/10.1021/acscatal.6b02979

Gandomkar, S., Żądło-Dobrowolska, A., & Kroutil, W. (2019). Extending designed linear biocatalytic cascades for organic synthesis. *ChemCatChem*, *11*(1), 225–243. https://doi.org/10.1002/cctc.201801063

Gernaey, K. V., Lantz, A. E., Tufvesson, P., Woodley, J. M., & Sin, G. (2010). Application of mechanistic models to fermentation and biocatalysis for next-generation processes. *Trends in Biotechnology*, *28*(7), 346–354. https://doi.org/10.1016/j.tibtech.2010.03.006

Giessmann, R. T., Krausch, N., Kaspar, F., Cruz Bournazou, M. N., Wagner, A., Neubauer, P., & Gimpel, M. (2019). Dynamic modelling of phosphorolytic cleavage catalyzed by pyrimidine-nucleoside phosphorylase. *Processes*, *7*(6), 380. https://doi.org/10.3390/pr7060380

Goedl, C., Schwarz, A., Minani, A., & Nidetzky, B. (2007). Recombinant sucrose phosphorylase from *Leuconostoc mesenteroides*: Characterization, kinetic studies of transglucosylation, and application of immobilised enzyme for production of α-D-glucose 1-phosphate. *Journal of Biotechnology*, *129*(1), 77–86. https://doi.org/10.1016/j.jbiotec.2006.11.019

Goldberg, K., Schroer, K., Lütz, S., & Liese, A. (2007). Biocatalytic ketone reduction—A powerful tool for the production of chiral alcohols—Part I: processes with isolated enzymes. *Applied Microbiology and Biotechnology*, *76*(2), 237–248. https://doi.org/10.1007/s00253-007-1002-0

Helleckes, L. M., Hemmerich, J., Wiechert, W., von Lieres, E., & Grünberger, A. (2023). Machine learning in bioprocess development: From promise to practice. *Trends in Biotechnology*, *41*(6), 817–835. https://doi.org/10.1016/j.tibtech.2022.10.010

Hold, C., Billerbeck, S., & Panke, S. (2016). Forward design of a complex enzyme cascade reaction. *Nature Communications*, *7*(1), 12971. https://doi.org/10.1038/ncomms12971

Hoops, S., Sahle, S., Gauges, R., Lee, C., Pahle, J., Simus, N., Singhal, M., Xu, L., Mendes, P., & Kummer, U. (2006). COPASI—A COmplex PAthway SImulator. *Bioinformatics*, *22*(24), 3067–3074. https://doi.org/10.1093/bioinformatics/btl485

Kara, S., & Rudroff, F. (2021). *Enzyme cascade design and modelling*, Springer International Publishing. https://doi.org/10.1007/978-3-030-65718-5.

Kaspar, F., Giessmann, R. T., Hellendahl, K. F., Neubauer, P., Wagner, A., & Gimpel, M. (2020). General principles for yield optimization of nucleoside phosphorylase-catalyzed transglycosylations. *ChemBioChem*, *21*(10), 1428–1432. https://doi.org/10.1002/cbic.201900740

Kitaoka, M., Sasaki, T., & Taniguchi, H. (1992a). Conversion of sucrose into cellobiose using sucrose phosphorylase, xylose isomerase and cellobiose phosphorylase. *Journal of the Japanese Society of Starch Science*, *39*(4), 281–283. https://doi.org/10.5458/jag1972.39.281

Kitaoka, M., Sasaki, T., & Taniguchi, H. (1992b). Synthetic reaction of *Cellvibrio gilvus* cellobiose phosphorylase. *The Journal of Biochemistry*, *112*(1), 40–44. https://doi.org/10.1093/oxfordjournals.jbchem.a123862

Klimacek, M., Sigg, A., & Nidetzky, B. (2020). On the donor substrate dependence of group-transfer reactions by hydrolytic enzymes: Insight from kinetic analysis of sucrose phosphorylase-catalyzed transglycosylation. *Biotechnology and Bioengineering*, *117*(10), 2933–2943. https://doi.org/10.1002/bit.27471

Klimacek, M., Zhong, C., & Nidetzky, B. (2021). Kinetic modeling of phosphorylase-catalyzed iterative β-1,4-glycosylation for degree of polymerization-controlled synthesis of soluble cello-oligosaccharides. *Biotechnology for Biofuels*, *14*(1), 134. https://doi.org/10.1186/s13068-021-01982-2

Kruschitz, A., & Nidetzky, B. (2020). Removal of glycerol from enzymatically produced 2-α-D-glucosyl-glycerol by discontinuous diafiltration. *Separation and Purification Technology*, *241*, 116749. https://doi.org/10.1016/j.seppur.2020.116749

Kuschmierz, L., Shen, L., Bräsen, C., Snoep, J., & Siebers, B. (2022). Workflows for optimization of enzyme cascades and whole cell catalysis based on enzyme kinetic characterization and pathway modelling. *Current Opinion in Biotechnology*, *74*, 55–60. https://doi.org/10.1016/j.copbio.2021.10.020

Lauterbach, S., Dienhart, H., Range, J., Malzacher, S., Spöring, J.-D., Rother, D., Pinto, M. F., Martins, P., Lagerman, C. E., Bommarius, A. S., Høst, A. V., Woodley, J. M., Ngubane, S., Kudanga, T., Bergmann, F. T., Rohwer, J. M., Iglezakis, D., Weidemann, A., Wittig, U., … Pleiss, J. (2023). EnzymeML: Seamless data flow and modeling of enzymatic data. *Nature Methods*, *20*(3), 400–402. https://doi.org/10.1038/s41592-022-01763-1

Lencastre Fernandes, R., Bodla, V. K., Carlquist, M., Heins, A.-L., Eliasson Lantz, A., Sin, G., & Gernaey, K. V. (2013). Applying mechanistic models in bioprocess development. In C.-F. Mandenius & N. J. Titchener-Hooker (Eds.), *Measurement, monitoring, modelling and control of bioprocesses* (pp. 137–166). Springer Berlin Heidelberg. https://doi.org/10.1007/10_2012_166

Liebermeister, W., & Klipp, E. (2006). Bringing metabolic networks to life: convenience rate law and thermodynamic constraints. *Theoretical Biology and Medical Modelling*, *3*(1), 41. https://doi.org/10.1186/1742-4682-3-41

Mandenius, C.-F., & Brundin, A. (2008). Bioprocess optimization using design-of-experiments methodology. *Biotechnology Progress*, *24*(6), 1191–1203. https://doi.org/10.1002/btpr.67

Mieyal, J. J., & Abeles, R. H. (1972). Disaccharide phosphorylases. In P. D. Boyer (Ed.), *The enzymes* (Vol. 7, pp. 515–532). Academic Press. https://doi.org/10.1016/S1874-6047(08)60461-8

Milker, S., Fink, M. J., Oberleitner, N., Ressmann, A. K., Bornscheuer, U. T., Mihovilovic, M. D., & Rudroff, F. (2017). Kinetic modeling of an enzymatic redox cascade *in vivo* reveals bottlenecks caused by cofactors. *ChemCatChem*, *9*(17), 3420–3427. https://doi.org/10.1002/cctc.201700573

Mirza, O., Skov, L. K., Sprogøe, D., van den Broek, L. A. M., Beldman, G., Kastrup, J. S., & Gajhede, M. (2006). Structural rearrangements of sucrose phosphorylase from *Bifidobacterium adolescentis* during sucrose conversion. *Journal of Biological Chemistry*, *281*(46), 35576–35584. https://doi.org/10.1074/jbc.M605611200

Nazor, J., Liu, J., & Huisman, G. (2021). Enzyme evolution for industrial biocatalytic cascades. *Current Opinion in Biotechnology*, *69*, 182–190. https://doi.org/10.1016/j.copbio.2020.12.013

Nidetzky, B., Eis, C., & Albert, M. (2000). Role of non-covalent enzyme-substrate interactions in the reaction catalysed by cellobiose phosphorylase from *Cellulomonas uda*. *Biochemical Journal*, *351*(Pt 3), 649–659. https://doi.org/10.1042/bj3510649

Nidetzky, B., Griessler, R., Schwarz, A., & Splechtna, B. (2004). Cellobiose phosphorylase from *Cellulomonas uda*: Gene cloning and expression in *Escherichia coli*, and application of the recombinant enzyme in a 'glycosynthase-type' reaction. *Journal of Molecular Catalysis B: Enzymatic*, *29*(1), 241–248. https://doi.org/10.1016/j.molcatb.2003.11.014

Petroll, K., Kopp, D., Care, A., Bergquist, P. L., & Sunna, A. (2019). Tools and strategies for constructing cell-free enzyme pathways. *Biotechnology Advances*, *37*(1), 91–108. https://doi.org/10.1016/j.biotechadv.2018.11.007

Pfeiffer, M., & Nidetzky, B. (2023). Biocatalytic cascade transformations for the synthesis of C-nucleosides and N-nucleoside analogs. *Current Opinion in Biotechnology*, *79*, 102873. https://doi.org/10.1016/j.copbio.2022.102873

Qi, P., You, C., & Zhang, Y. H. P. (2014). One-pot enzymatic conversion of sucrose to synthetic amylose by using enzyme cascades. *ACS Catalysis*, *4*(5), 1311–1317. https://doi.org/10.1021/cs400961a

Rajashekhara, E., Kitaoka, M., Kim, Y.-K., & Hayashi, K. (2002). Characterization of a cellobiose phosphorylase from a hyper-thermophilic eubacterium, *Thermotoga maritima* MSB8. *Bioscience, Biotechnology, and Biochemistry*, *66*(12), 2578–2586. https://doi.org/10.1271/bbb.66.2578

Rosenthal, K., Bornscheuer, U. T., & Lütz, S. (2022). Cascades of evolved enzymes for the synthesis of complex molecules. *Angewandte Chemie International Edition*, *61*(39), e202208358. https://doi.org/10.1002/anie.202208358

Rosenthal, K., & Lütz, S. (2018). Recent developments and challenges of biocatalytic processes in the pharmaceutical industry. *Current Opinion in Green and Sustainable Chemistry*, *11*, 58–64. https://doi.org/10.1016/j.cogsc.2018.03.015

Ruales-Salcedo, A. V., Higuita, J. C., Fontalvo, J., & Woodley, J. M. (2019). Design of enzymatic cascade processes for the production of low-priced chemicals. *Zeitschrift für Naturforschung C*, *74*(3–4), 77–84. https://doi.org/10.1515/znc-2018-0190

Sadino-Riquelme, M. C., Rivas, J., Jeison, D., Hayes, R. E., & Donoso-Bravo, A. (2020). Making sense of parameter estimation and model simulation in bioprocesses. *Biotechnology and Bioengineering*, *117*(5), 1357–1366. https://doi.org/10.1002/bit.27294

Schrittwieser, J. H., Velikogne, S., Hall, M., & Kroutil, W. (2018). Artificial biocatalytic linear cascades for preparation of organic molecules. *Chemical Reviews*, *118*(1), 270–348. https://doi.org/10.1021/acs.chemrev.7b00033

Schulze, M., & Schenkendorf, R. (2020). Robust model selection: Flatness-based optimal experimental design for a biocatalytic reaction. *Processes*, *8*(2), 190. https://doi.org/10.3390/pr8020190

Schwaiger, K. N., Voit, A., Dobiašová, H., Luley, C., Wiltschi, B., & Nidetzky, B. (2020). Plasmid design for tunable two-enzyme co-expression promotes whole-cell production of cellobiose. *Biotechnology Journal*, *15*(11), 2000063. https://doi.org/10.1002/biot.202000063

Schwaiger, K. N., Voit, A., Wiltschi, B., & Nidetzky, B. (2022). Engineering cascade biocatalysis in whole cells for bottom-up synthesis of cello-oligosaccharides: flux control over three enzymatic steps enables soluble production. *Microbial Cell Factories*, *21*(1), 61. https://doi.org/10.1186/s12934-022-01781-w

Schwarz, A., Goedl, C., Minani, A., & Nidetzky, B. (2007). Trehalose phosphorylase from *Pleurotus ostreatus*: Characterization and stabilization by covalent modification, and application for the synthesis of α,α-trehalose. *Journal of Biotechnology*, *129*(1), 140–150. https://doi.org/10.1016/j.jbiotec.2006.11.022

Sheldon, R. A., & Brady, D. (2019). Broadening the scope of biocatalysis in sustainable organic synthesis. *Chemsuschem*, *12*(13), 2859–2881. https://doi.org/10.1002/cssc.201900351

Siedentop, R., Claaßen, C., Rother, D., Lütz, S., & Rosenthal, K. (2021). Getting the most out of enzyme cascades: Strategies to optimize *in vitro* multi-enzymatic reactions. *Catalysts*, *11*(10), 1183. https://doi.org/10.3390/catal11101183

Siedentop, R., & Rosenthal, K. (2022). Industrially relevant enzyme cascades for drug synthesis and their ecological assessment. *International Journal of Molecular Sciences*, *23*(7), 3605. https://doi.org/10.3390/ijms23073605

Siedentop, R., Siska, M., Möller, N., Lanzrath, H., von Lieres, E., Lütz, S., & Rosenthal, K. (2023). Bayesian optimization for an ATP-regenerating *in vitro* enzyme cascade. *Catalysts*, *13*(3), 468. https://doi.org/10.3390/catal13030468

Sigg, A., Klimacek, M., & Nidetzky, B. (2021). Three-level hybrid modeling for systematic optimization of biocatalytic synthesis: α-glucosyl glycerol production by enzymatic trans-glycosylation from sucrose. *Biotechnology and Bioengineering*, *118*(10), 4028–4040. https://doi.org/10.1002/bit.27878

Sigg, A., Klimacek, M., & Nidetzky, B. (2023). Pushing the boundaries of phosphorylase cascade reaction for cellobiose production II: Model-based optimization. Biotechnology and Bioengineering. https://doi.org/10.1002/bit.28601

Sperl, J. M., & Sieber, V. (2018). Multienzyme cascade reactions—Status and recent advances. *ACS Catalysis*, *8*(3), 2385–2396. https://doi.org/10.1021/acscatal.7b03440

Sun, S., Wei, X., Zhou, X., & You, C. (2021). Construction of an artificial *in vitro* synthetic enzymatic platform for upgrading low-cost starch to value-added disaccharides. *Journal of Agricultural and Food Chemistry*, *69*(1), 302–314. https://doi.org/10.1021/acs.jafc.0c06936

Teshima, M., Willers, V. P., & Sieber, V. (2023). Cell-free enzyme cascades—Application and transition from development to industrial implementation. *Current Opinion in Biotechnology*, *79*, 102868. https://doi.org/10.1016/j.copbio.2022.102868

Ubiparip, Z., De Doncker, M., Beerens, K., Franceus, J., & Desmet, T. (2021). β-glucan phosphorylases in carbohydrate synthesis. *Applied Microbiology and Biotechnology*, *105*(10), 4073–4087. https://doi.org/10.1007/s00253-021-11320-z

Ubiparip, Z., Moreno, D. S., Beerens, K., & Desmet, T. (2020). Engineering of cellobiose phosphorylase for the defined synthesis of cellotriose. *Applied Microbiology and Biotechnology*, *104*(19), 8327–8337. https://doi.org/10.1007/s00253-020-10820-8

Verhaeghe, T., Diricks, M., Aerts, D., Soetaert, W., & Desmet, T. (2013). Mapping the acceptor site of sucrose phosphorylase from *Bifidobacterium adolescentis* by alanine scanning. *Journal of Molecular Catalysis B: Enzymatic*, *96*, 81–88. https://doi.org/10.1016/j.molcatb.2013.06.014

Villegas-Torres, M. F., Ward, J. M., & Baganz, F. (2018). Optimisation of enzyme cascades for chiral amino alcohol synthesis in aid of host cell integration using a statistical experimental design approach. *Journal of Biotechnology*, *281*, 150–160. https://doi.org/10.1016/j.jbiotec.2018.07.014

Vyas, A., & Nidetzky, B. (2023). Energetics of the glycosyl transfer reactions of sucrose phosphorylase. *Biochemistry*, *62*(12), 1953–1963. https://doi.org/10.1021/acs.biochem.3c00080

Waldmann, H., Gygax, D., Bednarski, M. D., Randall Shangraw, W., & Whitesides, G. M. (1986). The enzymic utilization of sucrose in the synthesis of amylose and derivatives of amylose, using phosphorylases. *Carbohydrate Research*, *157*, c4–c7. https://doi.org/10.1016/0008-6215(86)85078-9

Wang, Y., Ren, H., & Zhao, H. (2018). Expanding the boundary of biocatalysis: Design and optimization of in vitro tandem catalytic reactions for biochemical production. *Critical Reviews in Biochemistry and Molecular Biology*, *53*(2), 115–129. https://doi.org/10.1080/10409238.2018.1431201

Wildberger, P., Luley-Goedl, C., & Nidetzky, B. (2011). Aromatic interactions at the catalytic subsite of sucrose phosphorylase: Their roles in enzymatic glucosyl transfer probed with Phe52→Ala and Phe52→Asn mutants. *FEBS Letters*, *585*(3), 499–504. https://doi.org/10.1016/j.febslet.2010.12.041

Wu, S., Snajdrova, R., Moore, J. C., Baldenius, K., & Bornscheuer, U. T. (2021). Biocatalysis: Enzymatic synthesis for industrial applications. *Angewandte Chemie International Edition*, *60*(1), 88–119. https://doi.org/10.1002/anie.202006648

Zhang, T., Yang, J., Tian, C., Ren, C., Chen, P., Men, Y., & Sun, Y. (2020). High-yield biosynthesis of glucosylglycerol through coupling phosphorolysis and transglycosylation reactions. *Journal of Agricultural and Food Chemistry*, *68*(51), 15249–15256. https://doi.org/10.1021/acs.jafc.0c04851

Zhong, C., Luley-Goedl, C., & Nidetzky, B. (2019). Product solubility control in cellooligosaccharide production by coupled cellobiose and cellodextrin phosphorylase. *Biotechnology and Bioengineering*, *116*(9), 2146–2155. https://doi.org/10.1002/bit.27008

Zhong, C., & Nidetzky, B. (2020). Three-enzyme phosphorylase cascade for integrated production of short-chain cellodextrins. *Biotechnology Journal*, *15*(3), 1900349. https://doi.org/10.1002/biot.201900349

Zhong, C., Ukowitz, C., Domig, K. J., & Nidetzky, B. (2020). Short-Chain cello-oligosaccharides: Intensification and scale-up of their enzymatic production and selective growth promotion among probiotic bacteria. *Journal of Agricultural and Food Chemistry*, *68*(32), 8557–8567. https://doi.org/10.1021/acs.jafc.0c02660

Zhong, C., Wei, P., & Zhang, Y.-H. P. (2017). A kinetic model of one-pot rapid biotransformation of cellobiose from sucrose catalyzed by three thermophilic enzymes. *Chemical Engineering Science*, *161*, 159–166. https://doi.org/10.1016/j.ces.2016.11.047

SUPPORTING INFORMATION

Additional supporting information can be found online in the Supporting Information section at the end of this article.

How to cite this article: Sigg, A., Klimacek, M., & Nidetzky, B. (2024). Pushing the boundaries of phosphorylase cascade reaction for cellobiose production I: Kinetic model development. *Biotechnology and Bioengineering*, *121*, 580–592. https://doi.org/10.1002/bit.28602